

# Origin of the Laleaua Albă dacite (Baia Sprie volcanic area and Au-Pb-Zn ore district, Romania): evidence from study of melt inclusions

Vladimir B. Naumov<sup>1</sup>, Vladimir A. Kovalenker<sup>2</sup>, Gheorghe Damian<sup>3, 4</sup>,  
Sergei S. Abramov<sup>2</sup>, Maria L. Tolstykh<sup>1</sup>, Vsevolod Yu. Prokofiev<sup>2</sup>,  
Floarea Damian<sup>3</sup>, Ioan Seghedi<sup>5</sup>

<sup>1</sup>Vernadsky Institute of Geochemistry and Analytical Chemistry, Russian Academy of Sciences, (GEOKHI RAS), Moscow, Russia

<sup>2</sup>Institute of Geology of Ore Deposits, Petrography, Mineralogy and Geochemistry, Russian Academy of Sciences, (IGEM RAS), Moscow, Russia

<sup>3</sup>Tech Univ Cluj Napoca, North University Center of Baia Mare, Baia Mare, Romania

<sup>5</sup>Department of Geology, "Alexandru Ioan Cuza" University of Iasi, Iasi, Romania

<sup>4</sup>Institute of Geodynamics, Romanian Academy, Bucharest, Romania

Crystal inclusions (plagioclase, biotite, magnetite) and melt inclusions were studied in minerals of the Laleaua Albă dacite (Baia Sprie, Romania). Electron microprobe analysis of 29 melt inclusions in the plagioclase, K-feldspar, and quartz confirm that crystallization of these minerals took place from typical silicic melts enriched in potassium relative to sodium ( $K_2O/Na_2O = 1.5$ ). The sum of the petrogenic components is 92–99 wt%. This points to a possible change in water content from 8 to 1 wt% during crystallization of phenocrysts. According to ion microprobe analysis of 11 melt inclusions, the minimum water content is 0.5 wt%, and the maximum water content is 6.1 wt%. The presence of high-density water fluid segregation in one of the melt inclusions suggests that the primary water content in the melt could reach 84 wt%. Ion microprobe data revealed a high concentration of Cu (up to 1260 ppm) as well as higher U content (from 5.0 to 14.3 ppm; average 11.5 ppm) in some melt inclusions as compared to the average U contents in silicic melts (2.7 ppm in island-arc settings and 7.9 ppm in continental rift settings). Chondrite-normalized trace-element patterns in melt inclusions suggest a complex genesis of the studied magmatic melts. Contents of some elements (for instance Sr and Ba) are close to those in island-arc melts, while others (for instance Th, U, and Eu) resemble those in melts of continental settings.

Key words: melt inclusions, silicic melts, volatile components, trace elements, Romania

## Introduction

Melt-inclusion studies of phenocrysts from ultramafic to felsic magmatic rocks have recently become an important tool for better understanding magma genesis

Addresses: V. B. Naumov, M. L. Tolstykh: e-mail: naumov@geokhi.ru

V. A. Kovalenker, S. S. Abramov, V. Y. Prokofiev: e-mail: kva@igem.ru

G. Damian: 20A Carol I Boulevard, 700505 Iasi, Romania; e-mail: damgeo@ubm.ro

F. Damian: e-mail: loricadamian@ubm.ro

I. Seghedi: e-mail: seghedi@geodin.ro

Received: October 21, 2013, accepted: May 9, 2014

(e.g. Frezzotti 2001; Lukács et al. 2005). In recent years such studies, focused on magmatic minerals, have also been applied to substantiate the relationship of ore mineralization to magmatic processes (e.g. Naumov et al. 1993, 2010a; Kovalenker et al. 1999, 2006; Prokofiev et al. 1999; Harris et al. 2003; Halter et al. 2004, 2005; Wallier et al. 2006; Davidson and Kamenetsky 2007; etc.). Such studies lead to a better understanding of magma generation, fractionation and emplacement at the surface/subsurface levels, as well as to the processes responsible for enrichment of magmas in elements essential for ore formation (ligands, gases and metals). Parental magmas of felsic rocks are usually characterized by the presence of abundant phenocrysts that in most cases contain melt inclusions considered to be primary, since they were trapped during the growth of host crystals. They are mainly represented by quartz and plagioclase.

In this article we discuss the origin of the Laleaua Albă (White Tulip) dike system exposed in the road quarry 9 km from the town of Baia Sprie (NW Romania) via a melt inclusion study, carried out on these rocks for the first time. They consist of dacite mingled with andesite cutting the complex Miocene volcanic andesitic volcanoclastic deposits surrounding the Baia Sprie area. Existing models on Laleaua Albă based on the study of petrography, major, trace and isotope rock and enclave composition suggest complex processes that include various sources: crystal fractionation from andesite magma, mixing and assimilation (e.g. Kovacs 2002; Kovacs et al. 2013). Kovacs and Fülöp (2010) suggest that mixing/mingling occurred between a basic magma similar in composition to mafic enclaves and an acid one that is suggested to be in equilibrium with K-feldspar, low-An plagioclase, quartz and biotite.

Since the exposed rocks are fresh, it is believed that emplacement of the dike system followed the formation of the nearby gold-polymetallic deposits of the Baia Sprie ore district. The K-Ar and Ar-Ar isotope ages of the Laleaua Albă rocks are among the youngest in the area (8.5–8.0 Ma; Pécskay et al. 2006), and are similar to the age (94–79 Ma; Kovacs et al. 1997) of the nearby ore deposits.

A previous study on melt inclusions in quartz and feldspar phenocrysts from the Dănești dacite extrusive dome situated south of Laleaua Albă was carried out (Grancea et al. 2003). The results suggest that the dacite was derived from K-rich metaluminous to slightly peraluminous melts with high Cl content (900–1700 ppm) and a wide range of dissolved water contents (1–5 wt%). According to Grancea et al. (2003) the compositions of melt inclusions suggest that en route to the low-pressure subsurface zone the magma was subjected to advanced fractional crystallization. This study led to three main conclusions: (1) low-pressure degassing during formation of the Dănești extrusive dome caused fluid enrichment in chlorine; (2) degassing fluids extracted metal chloride complexes from magmas, and (3) accumulation of the hydrothermal fluid during magma degassing was a necessary condition for generation of veined epithermal deposits in this district.

In this paper we report results of detailed petrographical and geochemical studies that include petrographical description and chemical compositions of dacitic rock from the Laleaua Albă rock-forming mineral composition (electron microprobe) and melt-inclusion composition (microthermometry, electron and ion microprobes), and compare the new data with already published results on the dacite, surrounding andesite and gabbro-dioritic enclaves (Kovacs 2002; Seghedi et al. 2004). We also carried out thermodynamic calculations to establish the PT conditions of primary magma generation. The composition of the microcrystals and melt inclusions in quartz crystals suggests that the parental melt was rhyolitic.

We propose here a more complex mechanism for the origin of the Laleaua Albă dacite based on the melt inclusion study that includes conditions of generation and composition of primary magmas.

#### ***Outline of the geodynamic setting, magmatism, and ore deposits of the Baia Mare district***

The Baia Mare volcanic area and ore district are part of the Oaş-Gutâi volcanic mountains and are situated at the northeastern boundary of the ALCAPA (Eastern Alpine-Western Carpathian-Northern Pannonian) block with the Tisza-Dacia block, near the border with the European Platform (e.g. Săndulescu et al. 1993; Márton et al. 2007; Schmid et al. 2008) (Fig. 1). They represent a complex segment of the Neogene–Quaternary Inner Carpathian volcanic region and border with the NW margin of the Transcarpathian Basin. The opposite rotations of the ALCAPA and Tisza-Dacia tectonic units into the Carpathian embayment are thought to be driven by the retreat of a kind of European lithospheric slab (e.g. Royden 1988). Their final emplacement was accompanied by substantial strike-slip movements, core complex extension, block rotations and extensive development of felsic and intermediate calc-alkaline volcanism (Fodor et al. 1999; Seghedi et al. 1998 2004; Soták et al. 2000; Csontos et al. 2002; Horváth et al. 2006; Pécskay et al. 2006; Lexa et al. 2010). Seghedi and Downes (2011) connected the magmatic activity from the Oaş and Gutâi Mountains (that include our studied area) with the extensional system development of the Transcarpathian Basin, assigned to the easternmost part of ALCAPA.

The magmatic activity in the Baia Mare volcanic area began in the Badenian (~14.8–15.1 Ma) with explosive volcanism, which is recorded in silicic tuff and ignimbrite deposits (Szakács et al. 2012). According to K-Ar dating this event was subsequently followed by extrusion (13.4–9 Ma) of basaltic andesites, dacites, and andesites, and small basaltic intrusions in the Sarmatian and Pannonian (8.0–6.9 Ma; Edelstein et al. 1992, 1993; Lang et al. 1994; Pécskay et al. 1995; 2006; Kovacs et al. 1997). Chiefly andesitic volcanism (14–7 Ma) in the Baia Mare ore district is linked to the moderate-K, calc-alkaline association with high LILE and LREE contents. Petrological and isotope data indicate their derivation from crustal-

contaminated, subduction-related mantle magmas (Kovacs 2002), and also from mixing of crustal-derived melts with mantle-derived melts (Seghedi et al. 2004; Seghedi and Downes 2011).

The development of magmatic rocks and associated ore deposits was spatially projected at depth to a hidden pluton 65 km long and 15 km wide (see inset, Fig. 1), the outlines of which coincide with the boundary of the ore district

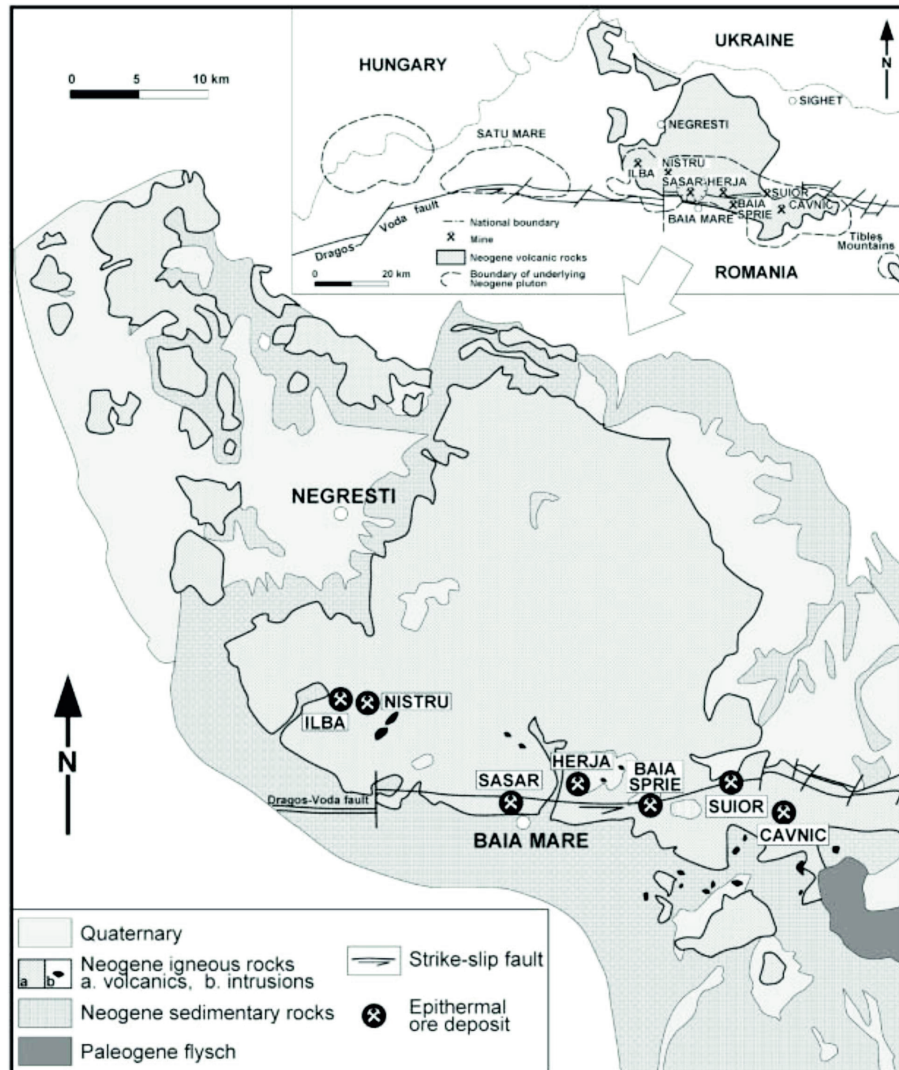


Fig. 1  
Schematic geologic map of the Baia Mare ore district and the main gold-polymetallic epithermal deposits. Inset shows the Dragoș Vodă deep-seated fault system and the outlines of a hidden pluton (according to geophysical data). After Grancea et al. 2003

(Borcoş 1994; Milesi et al. 1994; Mitchell 1996). Although this pluton is not exposed, its existence is confirmed on the basis of geophysical data (Crahmaliuc et al. 1995). The ore deposits are confined to the E–W fault system, which is traceable beneath Neogene volcanic rocks on the basis of excavations and prospecting drilling, as well as satellite images and gravity anomalies (Săndulescu et al. 1993).

Gold-polymetallic deposits of the Baia Mare ore district (Baia Sprie, Sasar, Nistru, Căvnic, Ilba, Herja, Suior, and others; Fig. 1) are situated in the Neogene calc-alkaline magmatic rocks, which intruded the basement of Lower Cambrian metamorphic rocks, the Paleogene Trans-Carpathian flysch sequence, and Neogene molasse sediments (Săndulescu 1988). Ore mineralization also shows a progressive younging from the west to the east: deposits located in the western part of the district (Ilba, Nistru and Săsar) were formed within 11.5–10 Ma, whereas those in the eastern part (Herja, Baia Sprie, Suior and Căvnic) define ages within 94–79 Ma (Kovács et al. 1997).

The considered deposits bear typical features (Simmons et al. 2005) of epithermal low-sulfidation ore-forming systems. According to numerous publications (Borcoş et al. 1995; Damian et al. 1995; Kovács et al. 1995 1997; etc.), the gold-polymetallic ores show various structures (banded, drusy, and less commonly disseminated and stockwork). A peculiar feature of the Baia Sprie, Căvnic, Săsar, and Suior deposits is the presence of remarkable brecciated pipe-like ore bodies, which point to strong phreatomagmatic explosions followed by hydrothermal activity and metal precipitation. Ore mineral assemblages include native elements (Au, Ag, Cu, As, and S), sulfides (pyrite, chalcopyrite, sphalerite, galena, antimonite), sulfosalts (tetrahedrite, jamesonite, bournonite, semseyite, pyrargyrite) and wolframates (wolframite, scheelite), and gangue minerals (quartz, adularia, clay minerals, carbonates, rhodonite, and barite). Hydrothermal alterations are dominated by propylitization and change from adularia-sericite, usually developed near silicification veins and argillic altered zones, with larger development within the veins.

Intrusive magmatism in the area is represented by subvolcanic and intravolcanic bodies, which are made up of microdiorite-andesite, quartz diorite, quartz monzonite, microgranodiorite-dacite, and tonalite (e.g. Kovács 2002). These intrusions played a significant role in the formation of the ore deposits.

## **Methods**

### *Petrologic and geochemical analytical techniques*

Five samples were investigated and 14 thin sections were made for petrographical investigations and determination of modal proportions.

Microprobe determinations of mineral composition were performed at the Institute of Experimental Mineralogy of RAS (Chernogolovka, Moscow region, by analyst K.V. Van). Analyses were carried out on Tescan Vega TS5130MM and

Tescan Vega XMU scanning electron microscopes equipped with INCAPentaFETx3 and INCAx-sight energy dispersive spectrometers, respectively. The scanning electron microscopes are equipped with the INCA Energy 350 system for X-ray spectral analysis. Measurements were carried out at accelerating voltage of 20 kV, beam current of 0.4–0.5 nA, and counting time of 70 s. Reference standards were as follows: quartz for Si, albite for Na, orthoclase for Na, orthoclase for K, wollastonite for Ca,  $\text{Al}_2\text{O}_3$  for Al, pyrite ( $\text{FeS}_2$ ) for S, GaP for P, MgO for Mg, fluorite ( $\text{CaF}_2$ ) for F, and pure metals for Ti, Fe, Mn, Cr, and Ni.

For investigation of inclusions, 0.3 mm-thick, double-polished thin sections (12) were prepared. The thin sections were examined microscopically to choose phenocrysts with melt inclusions. Crystalline inclusions and silicate glasses were analyzed using a "Cameca SX-100" microprobe (Vernadsky Institute of Geochemistry and Analytical Chemistry, Russian Academy of Sciences) under the following conditions: accelerating voltage of 15 kV, current of 30 nA, extended over areas of  $12 \times 12$  and  $5 \times 5$  mm for glasses. The analytical accuracy was 2 rel.% for element contents  $> 10$  wt%, 5 rel.% for 5–10 wt%, and 10 rel.% for element contents  $< 5$  wt%. Fluorine was determined on a TAP analyzer crystal ( $2d = 25.745$  Å) along an FK $\alpha$  line in an integral regime to avoid its interference with other elements during analysis. The standard reference sample was  $\text{MgF}_2$  as the most stable and compositionally suitable. The detection limit was 0.1 wt%, and the mean square deviation within the concentration range was no more than 19 rel.%.

Melt inclusions larger than 25  $\mu\text{m}$  in size were analyzed for  $\text{H}_2\text{O}$ , F, and trace elements by secondary ion mass spectrometry on an IMS-4f ion microprobe at the Yaroslavl Branch of the Physical Technical Institute (Yaroslavl, Russia) using technique described in Sobolev (1996); Nosova et al. (2002); Portnyagin et al. (2002).

### *Petrography, composition of rocks and minerals*

#### *Rock composition*

The subvolcanic Laleaua Albă dacite body is situated in the western part of the Baia Mare volcanic area, almost in the center of the Baia Sprie ore field, one of the largest in this area. The position of subvolcanic intrusion is shown in the geologic sketch of the area and the ore field (Fig. 2). The body is exposed in a quarry and has a vertically elongated dyke-like shape. It is markedly distinguished by its whitish color against dark host andesite and received its name due to its similarity to a tulip shape (Fig. 3). Two types of dacite were found. The first one is largely porphyritic and is made up of large quartz, feldspar, biotite, amphibole, and pyroxene crystals of strongly variable size (serial porphyritic texture) embedded in a microcrystalline groundmass. The second type is found near the contact with the host andesite and has an aphanitic groundmass consisting mainly of volcanic glass.

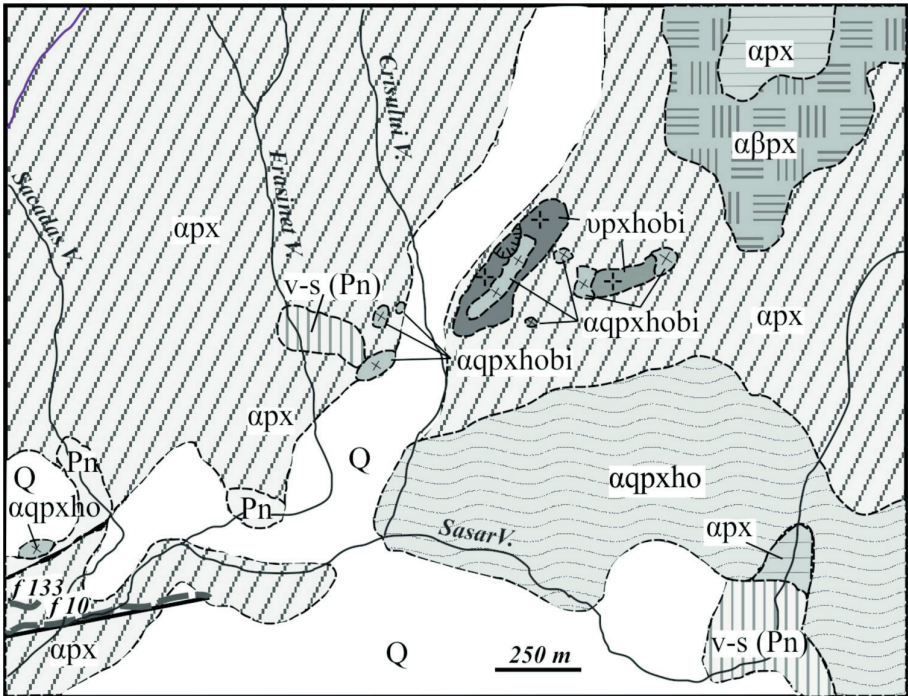


Fig. 2  
Simplified geologic sketch of the site of the Baia Sprie ore field with an exposure of the Laleaua Albă dacite. Compiled by G. Damian



Fig. 3  
The Laleaua Albă dike-like dacitic body (light) among andesite. Quarry on the road between Baia Sprie and Sigetu Marmati

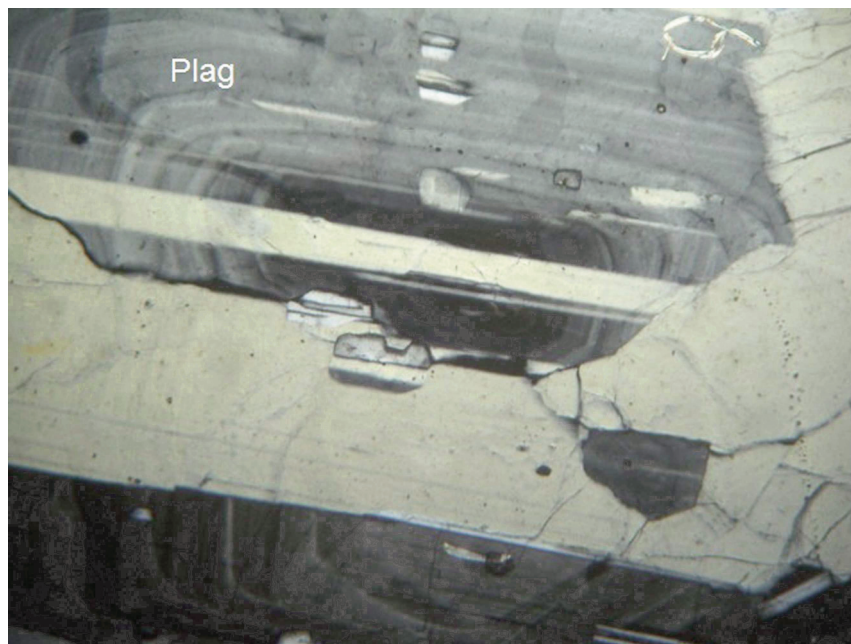


Fig. 4  
Zoned and twinned plagioclase crystals (Plag), N||,  $\times 30$

The rock contains abundant phenocrysts of feldspar (20–30%), quartz (7%), amphibole (7%), biotite (6%), pyroxene (3%), opaque minerals, and apatite embedded in a microcrystalline or aphanitic groundmass (up to 50%). Plagioclase varies in size from a few mm to microlite grains (0.01 mm). It is twinned (Fig. 4) and varies in composition from oligoclase through andesine to labradorite ( $An_{15}$ – $An_{60}$ ). Kovacs and Fülöp (2010) also describe large (up to 5 cm) K-feldspar (sanidine), with typical Karlsbad twins in the dacite.

The largest quartz phenocrysts reach 2–3 mm in size. The crystals are often strongly corroded and fissured, sometimes showing optical heterogeneity (Fig. 5). Mafic minerals are dominated by biotite and hornblende, with pyroxene and Titanomagnetite representing no more than 2–4%.

Biotite forms lamellar and tabular crystals. Together with secondary chlorite it is also observed as rims around and after amphibole (Fig. 6) represented by common hornblende. Pyroxenes (augite and, to lesser extent, hypersthene; Fig. 7) are present as euhedral and hypidiomorphic crystals, clusters, or as mafic inclusions. Pyroxenes were also described in reaction coronas surrounding quartz crystals, but only in the surrounding andesite (Kovacs 2002).

Fig. 5  
Corroded quartz  
phenocryst (Qz), N||,  $\times 30$

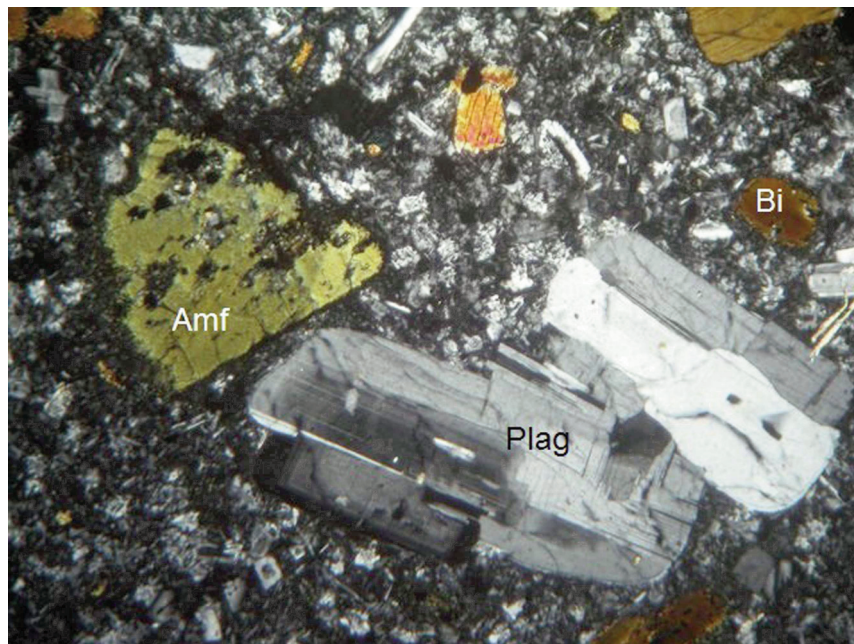


Fig. 6  
Phenocrysts of amphibole (Amf), biotite (Bi), and plagioclase (Plag) in a microcrystalline groundmass.  
N||,  $\times 30$

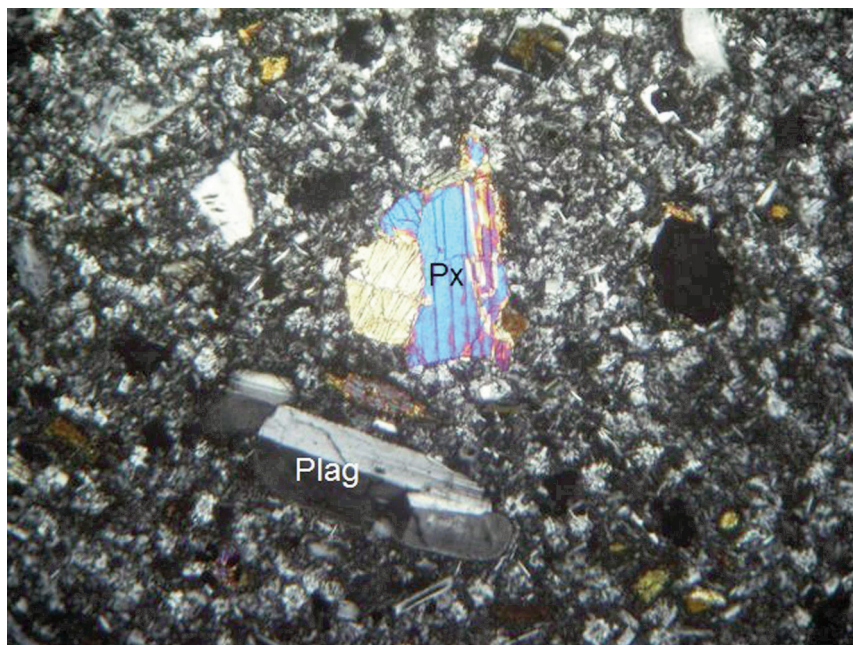


Fig. 7  
Phenocrysts of pyroxene (Px) and plagioclase (Plag) in a microcrystalline groundmass. N ||,  $\times 30$

The dacites often contain xenoliths of basic rocks up to 30 cm in size, which are distinguished by dark color as compared to dacite (Fig. 8). They have dioritic or gabbroic composition and consist mainly of plagioclase (48%) and amphiboles (36%) with subordinate biotite and pyroxene (for diorite) (Fig. 9), or of amphiboles and pyroxenes with subordinate plagioclase, biotite, and spinel (for gabbro).

The andesite that hosts the dacitic dike consists of scarce microcrystals of plagioclase, quartz, pyroxene, amphibole, and biotite in an aphanitic groundmass (Fig. 10).

#### *Petrography and geochemistry of rock and minerals*

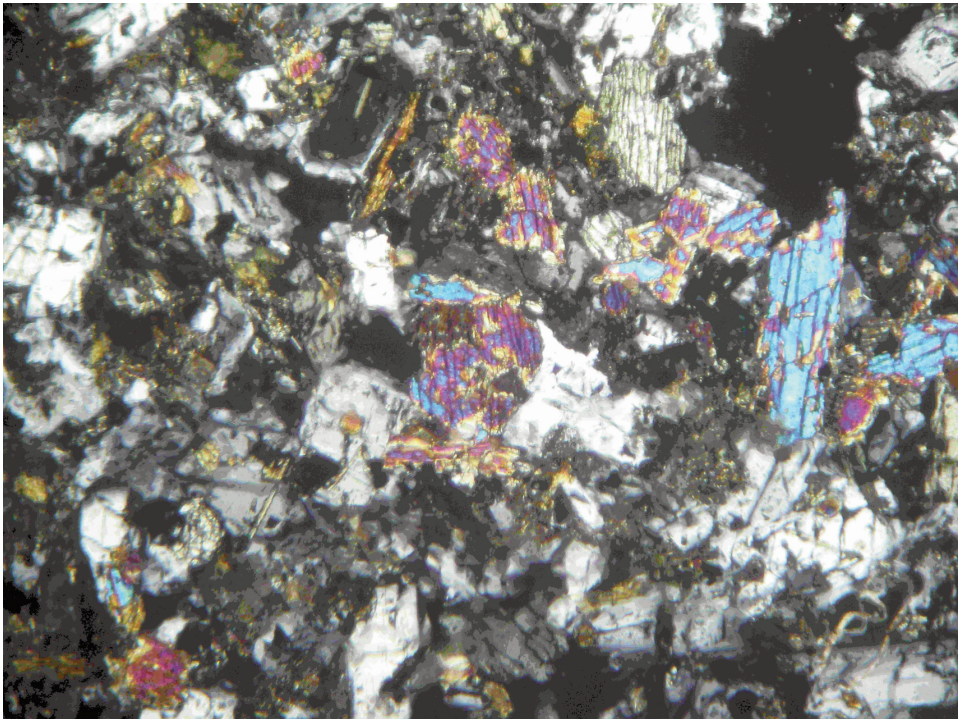
The Laleaua Albă subvolcanic body has dacitic composition (Table 1, analysis 1), similar to data published by Kovacs (2002). The chemical composition of phenocrysts is shown in Tables 1 and 2.

Clinopyroxene (augite with Mg# 83%) is present as poikilitic inclusions in phenocrysts of amphibole of a hastingsite composition. A peculiar feature of the

Fig. 8 →  
Diorite xenolith in  
dacite



Fig. 9 ↓  
Plagioclase,  
amphibole, and  
small amounts of  
biotite and pyroxene.  
Microphotos of a  
diorite xenolith in  
dacite. N||, × 30



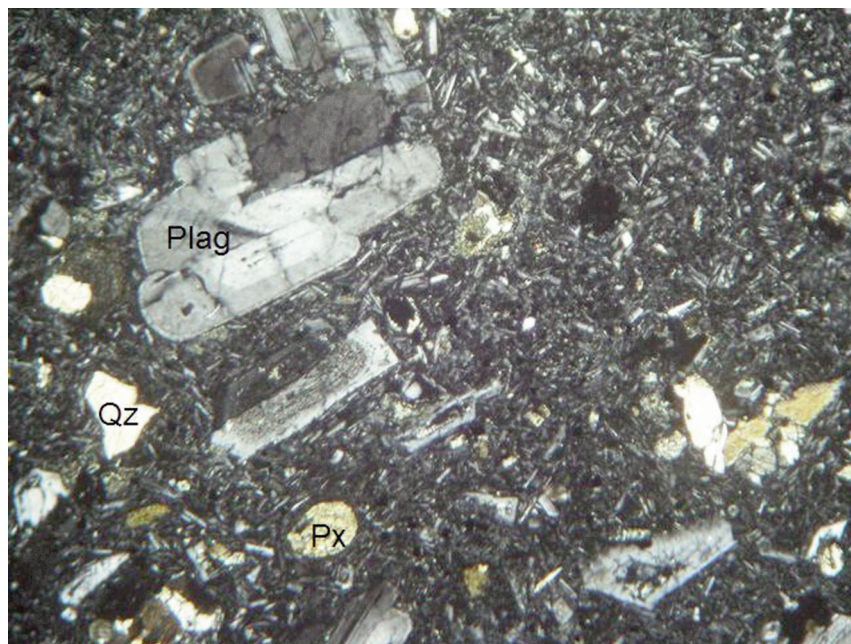


Fig. 10  
Quartz andesite: inclusions of quartz (Qz), pyroxene (Px), and plagioclase (Plag) in a microcrystalline groundmass. N||,  $\times 30$

amphibole and biotite phenocrysts is the presence of opacite rims consisting of opaque material and Ti-magnetite (black type of opacite rims according to Garcia and Jacobson 1979). Orthopyroxene is scarce among phenocrysts and more often occurs as small grains in the groundmass, but unlike amphibole and biotite, the orthopyroxene phenocrysts lack opacite rims.

Noteworthy is the presence of irregularly shaped polymineral microgranular inclusions (0.3–0.5 mm across). The inclusions consist of plagioclase, clinopyroxene, amphibole, and abundant opaque minerals (Ti-magnetite). In some inclusions the grain size and content of opaque material increases toward the core.

Phenocrysts of plagioclase, amphibole, and orthopyroxene are zoned. Most of plagioclase phenocrysts (Fig. 11) consist of three well-pronounced zones: core  $An_{65-64}$ , intermediate zone of  $An_{56}$  composition with a porous rim (sieve structure), and a narrow margin of increasingly calcic composition  $An_{66}$ . Hornblende phenocryst (Fig. 6) with Ti-magnetite inclusions shows core to rim variations of Mg# from 0.65 to 0.70–0.77. Orthopyroxene has an almost constant composition in the core, transitional zone, and rim. The groundmass of the rock

Table 1  
Chemical composition (wt%) of the Laleaua Albă dacite and minerals

Component	1	2	3	4	5	6	7	8	9	10	11	12	13	14	15
SiO <sub>2</sub>	67.72	49.75	56.31	58.89	57.06	63.17	52.34	49.00	48.95	52.06	48.25	0.77	0.27	0.40	0.06
TiO <sub>2</sub>	0.43	0.01	0.10	0.10	0.00	0.00	0.09	0.03	0.20	0.14	0.70	5.89	6.52	8.82	8.66
Al <sub>2</sub> O <sub>3</sub>	14.65	28.35	25.34	24.34	23.73	17.84	1.20	2.60	3.12	1.50	3.85	4.90	1.94	4.32	4.94
FeO	3.82	0.44	0.49	0.28	0.81	0.10	19.21	26.64	26.26	22.03	7.86	79.82	86.15	82.23	81.93
MnO	0.09	0.06	0.00	0.00	0.10	0.27	1.72	0.81	0.96	0.55	0.00	0.69	0.58	0.44	0.61
MgO	1.42	0.09	0.05	0.00	0.04	0.00	21.96	18.66	17.95	21.31	13.15	2.10	1.27	2.36	2.71
CaO	3.62	13.52	9.44	6.87	7.10	0.38	1.29	0.76	0.49	1.13	22.80	0.43	0.15	0.18	0.10
Na <sub>2</sub> O	3.10	3.47	5.78	6.58	6.10	3.08	0.32	0.08	0.07	0.17	0.22	-	-	-	-
K <sub>2</sub> O	3.51	0.25	0.50	1.21	1.54	11.43	0.00	0.04	0.05	0.04	0.00	-	-	-	-
Sum	99.64	95.94	98.01	98.27	96.48	96.27	98.13	98.62	98.05	98.93	96.83	94.60	96.88	98.75	99.01

Note: 1 – rock, Fe as Fe<sub>2</sub>O<sub>3</sub>, given amount P<sub>2</sub>O<sub>5</sub> = 0.13 and LOI = 1.15; 2–5 – plagioclase; 6 – K-feldspar; 7–10 – orthopyroxene (8 – center, 9 – medium, 10 – margin); 11 – clinopyroxene; 12–15 – magnetite.

is made up of a quartz-feldspathic aggregate with inclusions of fine orthopyroxene and Ti-magnetite. It has micro-grained aplitic-like, locally granophyric texture and contains plagioclase An<sub>35–46</sub> and K-feldspar Ab<sub>28</sub>Or<sub>70</sub>.

Table 2  
Chemical composition (wt%) of amphibole and biotite from the Laleaua Albă dacite

Component	1	2	3	4	5	6	7	8	9	10	11
SiO <sub>2</sub>	38.28	39.46	39.51	39.52	39.85	39.70	39.76	38.65	39.26	35.03	35.52
TiO <sub>2</sub>	2.62	2.72	2.70	3.19	2.15	3.08	2.83	2.61	2.43	4.75	5.23
Al <sub>2</sub> O <sub>3</sub>	13.18	13.34	12.89	11.64	11.87	12.32	11.71	12.70	12.26	12.17	12.55
FeO	13.79	9.82	10.17	11.74	13.95	13.00	12.59	16.10	15.05	15.20	17.35
MnO	0.17	0.03	0.13	0.07	0.16	0.06	0.15	0.61	0.40	0.16	0.33
MgO	11.10	13.28	13.53	12.44	11.93	12.65	11.67	10.62	11.19	13.09	12.75
CaO	11.62	11.56	11.86	11.75	11.34	11.82	11.47	11.51	11.31	0.07	0.09
Na <sub>2</sub> O	1.77	1.95	2.00	1.66	1.98	2.38	1.83	2.00	1.97	0.66	0.45
K <sub>2</sub> O	1.09	1.13	0.89	0.95	0.82	0.62	0.87	1.21	1.04	8.97	9.44
Cl	0.03	0.01	0.06	0.04	0.00	0.04	0.08	0.02	0.05	0.00	0.07
F	0.00	0.38	0.00	0.00	0.00	0.00	0.00	0.16	0.00	0.18	0.11
Sum	93.65	93.68	93.74	93.00	94.05	95.67	92.96	96.19	94.96	90.28	93.89

Note: 1–9 – amphibole; 10, 11 – biotite

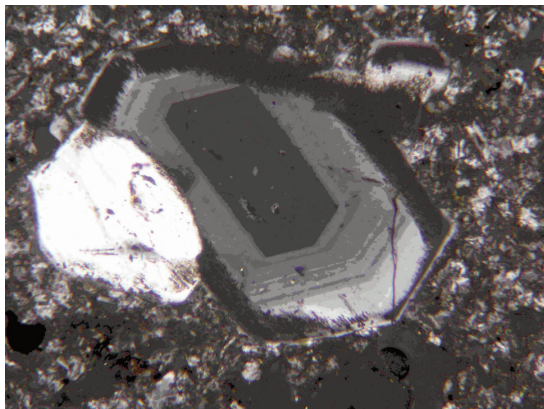


Fig. 11  
Zoned phenocryst of  
plagioclase in a dacitic  
groundmass

### *Melt and crystal inclusion study*

Quartz phenocrysts contain primary inclusions of silicate glass daughter crystals (quartz phenocrysts contain crystal and melt inclusions). Crystal inclusions (Table 3) are represented by plagioclase ( $An_{49-39}$ ), biotite (up to 0.41 wt% F and 0.19 wt% Cl), and magnetite ( $TiO_2 = 5.9-7.0$  wt%,  $MnO = 0.9-1.7$  wt%). It is very important to note that compositions of crystal inclusions in Qz have different compositions than phenocrysts in the rock. Melt inclusions consist of silicate glass and fluid phase (Fig. 12a–d). In one melt inclusion, the fluid phase at room temperature consists of liquid and gas phases (Fig. 12d).

The chemical composition of homogenized melt inclusions in plagioclase, quartz, and K-feldspar is listed in Table 4. We analyzed 29 inclusions. The  $SiO_2$  content in the melt varies from 68.3 to 75.5 wt%. The average composition of melt inclusions is as follows (in wt%): 72.34  $SiO_2$ , 0.07  $TiO_2$ , 12.58  $Al_2O_3$ , 0.60 FeO, 0.07 MnO, 0.07 MgO, 0.90 CaO, 3.50  $Na_2O$ , 5.13  $K_2O$ , 0.06  $P_2O_5$ , 0.12 Cl, 0.07 F, 0.01 S. These data indicate that phenocrysts crystallized from typical silicic melts with  $K_2O/Na_2O = 1.5$ .

The microprobe data have an average total of 95.52 wt%, suggesting an average water content of 4.5 wt% in melt. Yet the large variations of the components from 92 to 99 wt%, may suggest that the water content during crystallization of phenocryst changed from 8 to 1 wt%. From the diagrams (Fig. 13) of  $SiO_2$  vs contents of the sum of all other components as well as  $Al_2O_3$ , FeO, and  $K_2O$  it can be clearly seen that there is a direct correlation between  $SiO_2$  and sum of all components, and an absence of such correlation for other components. However, since it is not associated with a change in major element composition,  $H_2O$  could be lost from inclusions via proton diffusion. This is a particularly feasible process for slow cooling of inclusions in intrusive rocks (Audetat and Gunther 1999).

Figure 14 shows a melt inclusion in K-feldspar. In addition to gas bubble and silicate glass, there is a clear rim that developed around feldspar by cooling of the

Table 3  
Chemical composition (wt%) of crystalline inclusions in quartz from the Laleaua Albă dacite

Component	1	2	3	4	5	6	7	8	9	10	11
SiO <sub>2</sub>	51.82	55.42	58.40	58.94	35.88	36.69	33.55	35.95	0.16	0.14	0.10
TiO <sub>2</sub>	0.00	0.00	0.01	0.01	3.87	4.22	4.13	4.21	6.96	6.15	5.88
Al <sub>2</sub> O <sub>3</sub>	29.41	27.72	25.86	24.64	14.40	13.85	14.41	13.96	3.35	3.75	1.93
FeO	0.19	0.22	0.20	0.77	19.14	20.81	19.47	19.00	76.86	82.77	85.77
MnO	0.00	0.00	0.00	0.00	0.56	0.51	0.54	0.46	1.74	1.23	0.85
MgO	0.00	0.01	0.01	0.15	11.15	11.65	10.99	11.75	1.48	1.66	0.86
CaO	10.62	10.30	8.36	6.74	0.18	0.04	0.00	0.09	2.85	0.02	0.04
Na <sub>2</sub> O	5.83	5.91	6.79	6.73	0.50	0.47	0.48	0.48	0.04	0.00	0.03
K <sub>2</sub> O	0.34	0.40	0.54	1.11	8.28	8.95	8.91	8.47	0.05	0.03	0.01
Cl	0.00	0.00	0.00	0.05	0.16	0.15	0.14	0.19	0.06	0.01	0.00
F	0.00	0.00	0.00	0.00	0.34	0.34	0.41	0.41	0.23	0.11	0.00
Sum	98.21	99.98	100.17	99.14	94.46	97.68	93.03	94.97	93.78	95.87	95.47

Note: 1–4 – plagioclase, 5–8 – biotite, 9–11 – magnetite

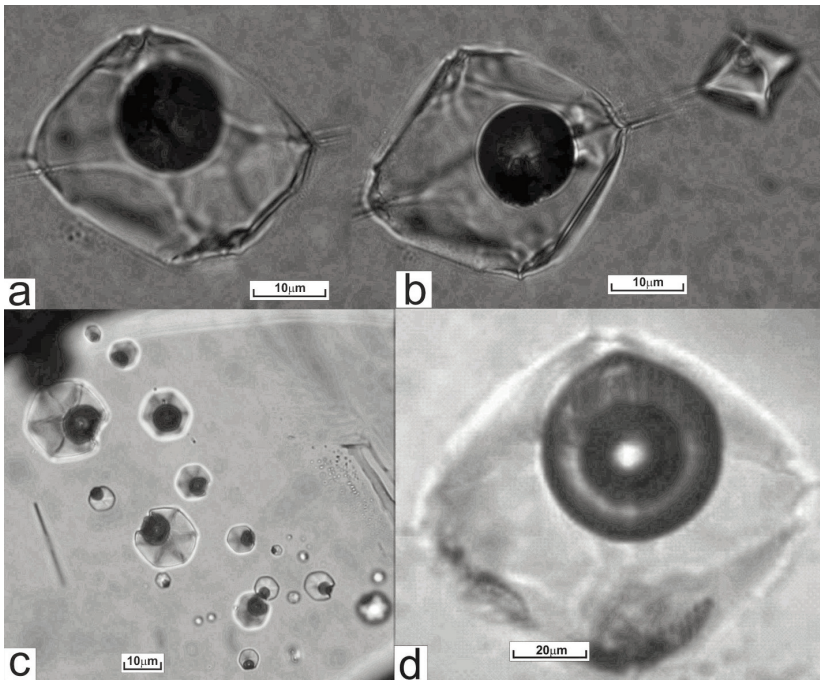


Fig. 12  
Melt inclusions in quartz phenocrysts. a–c: inclusions consisting of silicate glass and gas phase; d: two-phase fluid segregation in a melt inclusion consisting of gas phase and low-salinity aqueous solution (0.5 wt% NaCl equiv.) at room temperature. Fluid is homogenized into liquid at 225 °C

phenocryst. The composition of the rim of the host mineral should be taken into account to estimate the primary composition of the melt entrapped during mineral crystallization. Therefore the analysis of residual glass in this inclusion (analysis 29, Table 4) was recalculated (Table 4, analysis 29\*).

Ion microprobe analyses (water and trace elements) of 11 melt inclusions in quartz are presented in Table 5. The H<sub>2</sub>O content in the glass of melt inclusions varies from 0.5 to 6.1 wt%, averaging 3.5 wt%, which is very consistent with the

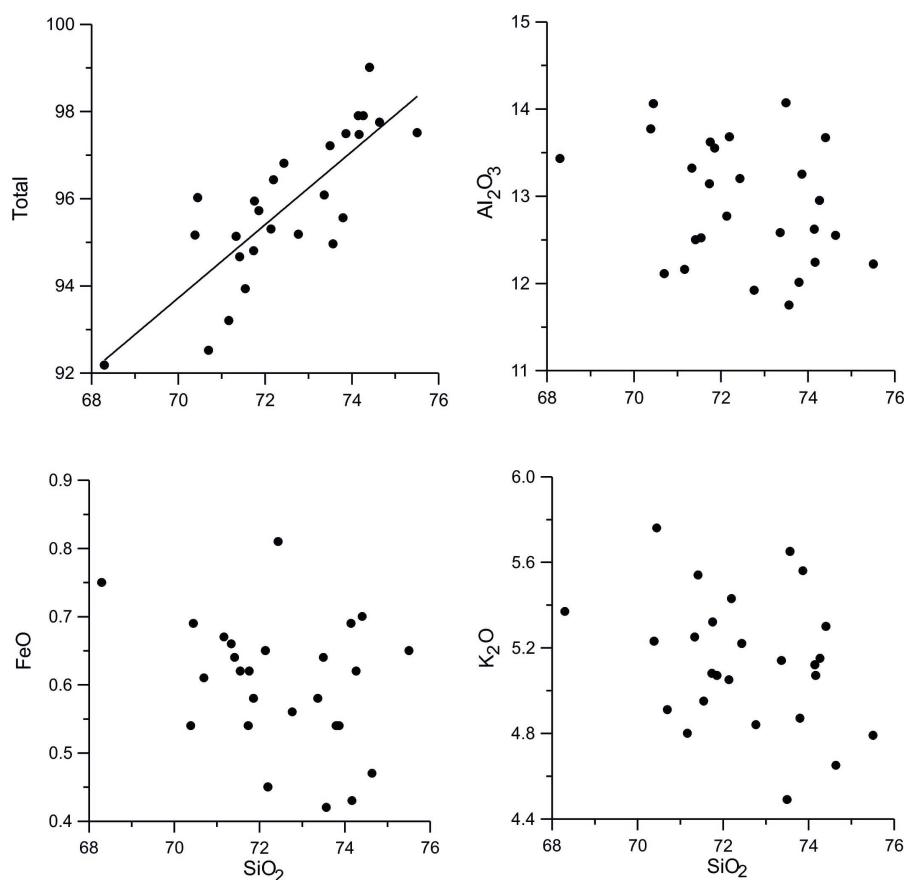
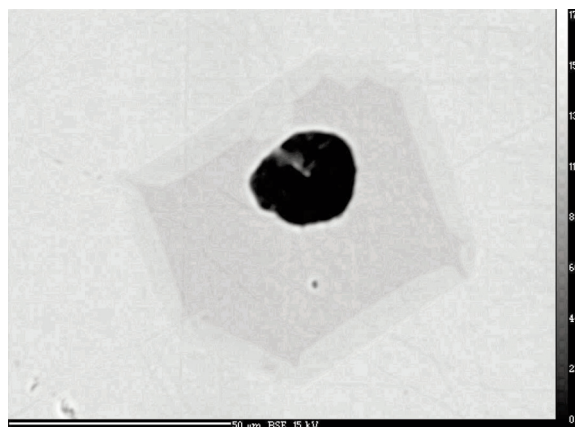


Fig. 13  
Diagrams showing variations of SiO<sub>2</sub> vs. sum of all components, and contents of Al<sub>2</sub>O<sub>3</sub>, FeO and K<sub>2</sub>O in melt inclusions from quartz phenocrysts

water contents presented above assumed by electron microprobe. Considering the high-density water of fluid segregation (Fig. 12d), the maximum water content in the melt was 84 wt%. Noteworthy is the high Cu content in some melt inclusions. The Cu concentrations are 345 ppm and 1260 ppm in the BM-6 and BM-4 inclusions. Inclusion BM-14 is also characterized by a higher Pb content (111 ppm) compared to other inclusions (10–36 ppm). Note also the higher U content

Fig. 14  
Melt inclusion in K-feldspar consisting of gas bubble, silicate glass, and feldspar rim that crystallized over the entire volume of inclusion on cooling of the phenocryst



(from 5.0 to 14.3 ppm, averaging 11.5 ppm) in the obtained analyses as compared to its average content in silicic melts (2.7 ppm in island arc settings and 79 ppm in continental rifts) (Naumov et al. 2010b).

The volume of the fluid phase of one melt inclusion in quartz is ~ 7 vol.% (Fig. 12d). According to cryometric measurements, at the ice melting temperature of  $-0.3\text{ }^{\circ}\text{C}$  the fluids corresponds to a low-salinity aqueous solution (0.5 wt% NaCl equiv.). The fluid inclusion was homogenized as liquid at  $225\text{ }^{\circ}\text{C}$ , which indicates the high density of the fluid phase ( $0.84\text{ g/cm}^3$ ) and, correspondingly, the high water pressure during quartz crystallization from magmatic melt. At a melt temperature of around  $800\text{ }^{\circ}\text{C}$  fluid pressure was no less than 8 kbar.

Primitive mantle and chondrite-normalized (Sun and McDonough 1989) trace element patterns for melt inclusions are shown in Fig. 15a, b, in comparison with existing whole rock analysis (Kovacs 2002) and UA34, the most primitive basalt in the nearby area considered to be of lithospheric mantle origin (Seghedi et al. 2001). With exception of K and U, which are enriched in melt inclusions, all other incompatible elements are either equal or strongly depleted compared to the whole rock and different from the basalt. The compositions show similarities to island-arc melts in terms of some elements (for instance Sr and Ba), and resemble melts of continental settings in terms of other elements (Th, U, and Eu), which suggests their complex genesis.

Major and trace element whole rock compositions for most of available volcanic rocks in from the Transcarpathian Basin area have been plotted (Downes et al.

Table 4  
The chemical composition (wt%) of melt inclusions in plagioclase (1, 2), quartz (3–28) and K-feldspar (29) from the Laleaua Albă dacite

No. inclusion	Component													Sum
	SiO <sub>2</sub>	TiO <sub>2</sub>	Al <sub>2</sub> O <sub>3</sub>	FeO	MnO	MgO	CaO	Na <sub>2</sub> O	K <sub>2</sub> O	P <sub>2</sub> O <sub>5</sub>	F	Cl	S	
1	68.51	0.11	16.76	0.45	0.06	0.05	3.24	5.99	3.19	0.05	0.00	0.08	0.00	98.49
2	72.62	0.19	13.42	0.75	0.01	0.13	2.51	3.98	3.71	0.06	0.00	0.10	0.01	97.49
3	68.30	0.07	13.43	0.75	0.04	0.05	0.74	3.24	5.37	0.00	0.04	0.15	-	92.18
4	70.39	0.06	13.77	0.54	0.11	0.09	0.85	3.80	5.23	0.13	0.06	0.13	0.00	95.16
5	70.45	0.06	14.06	0.69	0.06	0.07	0.89	3.70	5.76	0.02	0.16	0.10	0.00	96.02
6	70.70	0.04	12.11	0.61	0.04	0.05	0.66	3.27	4.91	0.01	0.00	0.12	-	92.52
7	71.17	0.01	12.16	0.67	0.01	0.10	0.72	3.36	4.80	0.00	0.08	0.12	-	93.20
8	71.34	0.07	13.32	0.66	0.12	0.00	0.84	3.26	5.25	0.01	0.14	0.12	0.00	95.13
9	71.42	0.09	12.50	0.64	0.10	0.06	0.64	3.52	5.54	0.02	0.00	0.13	0.00	94.66
10	71.55	0.06	12.52	0.62	0.06	0.06	0.69	3.32	4.95	0.00	0.00	0.10	-	93.93
11	71.74	0.06	13.14	0.54	0.12	0.07	0.80	3.14	5.08	0.00	0.00	0.11	0.00	94.80
12	71.76	0.07	13.62	0.62	0.07	0.08	0.84	3.32	5.32	0.11	0.00	0.11	0.02	95.94
13	71.86	0.05	13.55	0.58	0.08	0.08	0.82	3.36	5.07	0.14	0.00	0.12	0.01	95.72
14	72.14	0.12	12.77	0.65	0.11	0.06	0.77	3.33	5.05	0.06	0.09	0.15	-	95.30
15	72.20	0.04	13.68	0.45	0.04	0.08	0.69	3.34	5.43	0.21	0.12	0.15	0.00	96.43
16	72.44	0.10	13.20	0.81	0.06	0.06	0.76	3.71	5.22	0.07	0.20	0.17	0.01	96.81
17	72.77	0.06	11.92	0.56	0.03	0.09	0.93	3.86	4.84	0.00	0.00	0.12	0.00	95.18
18	73.37	0.08	12.58	0.58	0.04	0.09	0.65	3.34	5.14	0.00	0.11	0.10	-	96.08
19	73.50	0.09	14.07	0.64	0.09	0.10	0.85	3.13	4.49	0.10	0.04	0.10	0.01	97.21
20	73.57	0.06	11.75	0.42	0.05	0.04	0.51	2.81	5.65	0.04	0.00	0.06	0.00	94.96
21	73.80	0.03	12.01	0.54	0.11	0.05	0.65	3.21	4.87	0.06	0.14	0.09	-	95.56
22	73.87	0.08	13.25	0.54	0.07	0.05	0.75	3.06	5.56	0.00	0.14	0.12	-	97.49
23	74.15	0.09	12.62	0.69	0.06	0.09	0.78	3.80	5.12	0.03	0.34	0.12	0.01	97.90
24	74.17	0.06	12.24	0.43	0.04	0.09	0.91	4.10	5.07	0.03	0.20	0.10	0.03	97.47
25	74.27	0.07	12.95	0.62	0.08	0.06	0.71	3.73	5.15	0.14	0.01	0.10	0.01	97.90
26	74.41	0.07	13.67	0.70	0.08	0.08	0.81	3.67	5.30	0.02	0.04	0.14	0.02	99.01
27	74.64	0.05	12.55	0.47	0.08	0.08	0.97	4.07	4.65	0.06	0.00	0.13	0.00	97.75
28	75.51	0.09	12.22	0.65	0.07	0.09	0.72	2.98	4.79	0.12	0.17	0.09	0.01	97.51
29	75.89	0.09	9.07	0.79	0.03	0.09	0.45	2.00	5.02	0.12	0.10	0.21	0.01	93.87
29*	71.28	0.05	12.60	0.57	0.03	0.06	0.32	2.13	8.20	0.12	0.06	0.13	0.00	95.55

Note: 29 – residual glass after crystallization of the host mineral rims, 29\* – calculated composition of the melt, taking into account 60% residual glass and 40% rim feldspar

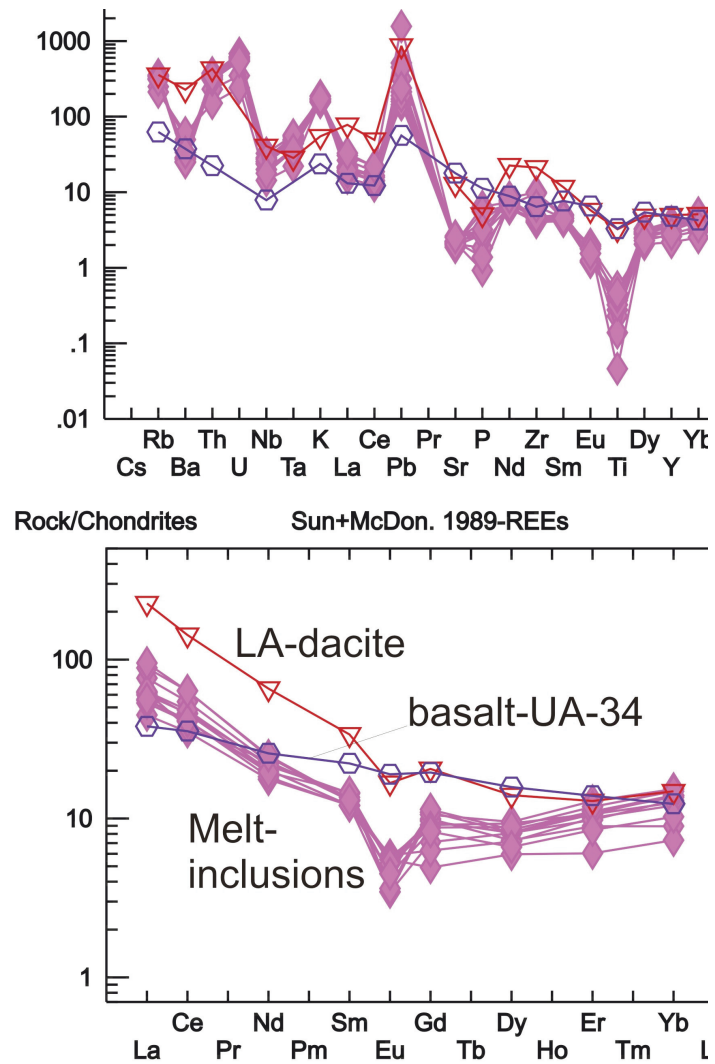


Fig. 15  
Primitive mantle and chondrite-normalized (Sun and McDonough 1989) trace element patterns for melt inclusions (filled diamonds), host dacite (open triangles) and UA-34 (open circle), a calc-alkaline basalt in the Transcarpathian Basin area (from Seghedi et al. 2001)

1995; Seghedi et al. 2001, 2004; Seghedi and Downes 2011), along with newly published data on quartz andesites in the Baia Mare region (Jurje et al. 2014) and available mafic enclave, andesite and dacite analyses of Laleaua Albă (Kovacs 2002; Seghedi et al. 2004) (Fig. 16). The diagrams expose higher values for Rb, Ba, Th, Pb, and La of the Laleaua Albă dacite, showing a different trend compared to all the other intermediate or felsic rocks. On the other hand the melt inclusion composition shows similarity with the whole rock composition of the Laleaua Albă dacite only for Rb and Th, but lower values for Ba, Zr, La, and Pb. Also, the melt inclusion composition regularly shows similarities with felsic calc-alkaline

Table 5  
The chemical composition (wt%), water and trace elements (ppm) content in the melt inclusions in the quartz from Laleaua Albă dacite

Component	BM-1	BM-2	BM-3	BM-4	BM-5	BM-6	BM-7	BM-8	BM-9	BM-10	BM-11
SiO <sub>2</sub>	73.57	74.64	71.42	72.14	73.80	73.37	71.17	75.15	75.27	75.51	73.44
TiO <sub>2</sub>	0.06	0.05	0.09	0.12	0.03	0.08	0.01	0.09	0.07	0.09	0.10
Al <sub>2</sub> O <sub>3</sub>	11.75	12.55	12.50	12.77	12.01	12.58	12.16	12.62	12.95	12.22	13.20
FeO	0.42	0.47	0.32	0.32	0.54	0.67	0.67	0.69	0.65	0.67	0.81
MnO	0.05	0.08	0.10	0.11	0.11	0.04	0.01	0.06	0.08	0.07	0.06
MgO	0.04	0.08	0.06	0.06	0.05	0.09	0.10	0.09	0.06	0.09	0.06
CaO	0.51	0.97	0.64	0.77	0.65	0.65	0.72	0.78	0.71	0.72	0.76
Na <sub>2</sub> O	2.81	4.07	3.52	3.33	3.21	3.34	3.36	2.30	2.73	2.98	2.71
K <sub>2</sub> O	5.65	4.65	5.54	5.05	4.87	5.14	4.80	5.12	5.15	4.79	5.22
P <sub>2</sub> O <sub>5</sub>	0.04	0.06	0.02	0.06	0.06	0.00	0.00	0.03	0.14	0.12	0.07
Cl	0.06	0.13	0.13	0.15	0.09	0.10	0.12	0.12	0.10	0.09	0.17
S	0.00	0.00	0.00	-	-	-	-	0.01	0.01	0.01	0.01
H <sub>2</sub> O	2.11	0.49	0.49	1.87	5.71	5.25	6.07	2.93	2.30	4.13	3.18
Sum	97.07	98.24	94.83	97.08	101.13	101.22	99.26	99.99	100.19	101.47	99.69
Li (ppm)	51.5	9.87	15.9	121	343	263	448	221	372	349	274
Be	1.60	1.10	0.29	1.13	2.83	3.14	2.93	2.93	3.10	3.30	1.70
B	49.9	34.4	0.74	33.4	73.5	71.1	90.7	88.7	76.7	78.1	53.3
F	173	201	7.8	340	159	400	180	202	193	178	134
Cr	1.07	0.68	0.85	-	5.94	7.31	3.82	0.72	1.24	0.52	7.73
V	4.81	5.09	3.78	13.6	5.24	9.99	3.89	4.28	4.10	4.02	5.86
Cu	8.56	55.2	21.3	1260	156	345	38.8	16.9	31.6	12.7	125
Rb	214	158	218	134	221	227	197	201	220	201	195
Sr	43.6	55.4	45.5	47.1	41.1	46.5	39.4	47.4	44.5	42.8	53.1
Y	13.7	11.8	16.7	9.89	14.2	18.4	16.1	16.8	16.5	16.0	12.7
Zr	44.6	45.6	53.3	112	47.5	53.7	51.3	50.3	52.9	108	73.6
Nb	18.0	14.2	20.1	10.2	18.2	23.3	17.0	16.8	20.3	19.4	12.7
Ba	178	347	194	424	173	190	174	199	201	175	234
La	10.6	18.1	14.6	21.0	13.1	14.7	12.6	14.2	14.9	13.3	22.5
Ce	21.5	33.2	27.9	38.9	25.4	23.0	24.9	28.1	29.4	25.2	38.8
Nd	8.22	10.6	9.47	11.4	8.54	10.7	9.45	10.3	10.0	9.14	11.6
Sm	1.85	2.08	1.84	1.97	1.84	1.99	1.85	2.19	2.21	2.23	2.00
Eu	0.26	0.30	0.20	0.32	0.34	0.33	0.32	0.20	0.21	0.30	0.26
Gd	2.25	2.04	1.46	1.01	1.29	1.87	1.98	2.17	2.34	1.80	1.70
Dy	2.07	1.85	2.05	1.51	1.82	2.36	2.06	2.42	2.16	2.24	1.68
Er	1.82	1.48	1.76	1.00	1.67	1.77	1.62	2.13	1.83	1.96	1.40
Yb	2.31	1.52	2.14	1.24	2.05	2.36	2.21	2.60	2.38	2.52	1.74
Hf	2.17	1.79	2.29	0.92	2.01	2.58	2.12	2.24	1.94	3.49	2.76
Ta	1.97	1.53	2.00	0.90	1.79	2.32	1.90	2.03	2.20	2.27	1.46
Pb	12.1	10.2	11.2	111	22.4	36.3	32.0	15.0	15.1	13.4	16.9
Th	28.4	19.6	26.4	12.8	26.0	27.4	31.5	32.0	30.1	30.1	29.5
U	12.9	7.32	11.8	5.02	11.4	14.2	12.3	14.3	13.0	12.8	11.3
Th/U	2.2	2.7	3.1	2.5	2.3	2.1	2.2	2.2	2.5	2.4	2.6
La/Yb	4.6	12	6.8	17	6.4	6.2	5.7	5.5	6.3	5.3	13

rocks already suggested to have a crustal origin (e.g., Seghedi and Downes 2011). In the diagrams there is an obvious gap between felsic and intermediate calc-alkaline rocks, and the felsic rocks do not follow the compositional trend of enrichment of the intermediate rocks in elements other than  $\text{SiO}_2$  (Fig. 16).

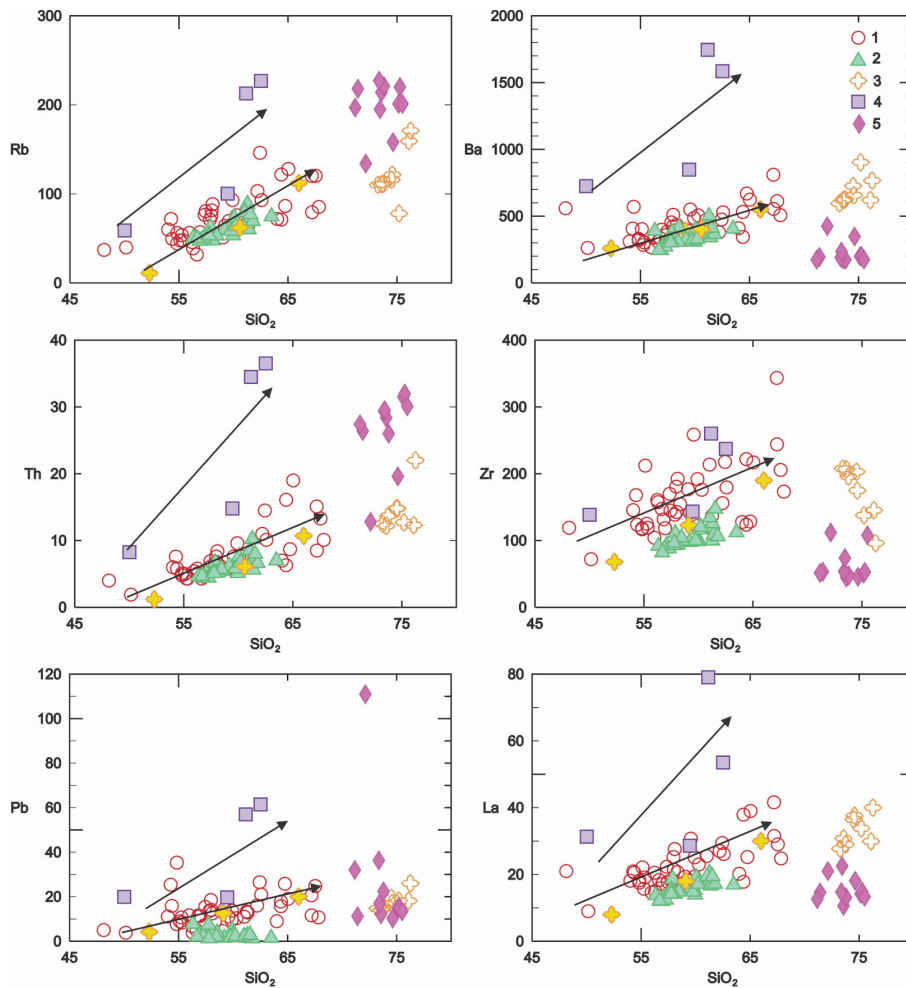


Fig. 16

Whole rock and melt inclusion  $\text{SiO}_2$  vs trace element compositions (Rb, Th, Pb, Ba, Zr and La) for most of the available volcanic rocks in the Transcarpathian Basin area; newly published data on quartz andesite in Baia Mare region and Laleaua Albă rocks. Two components mixing between mafic enclave and average melt inclusion is shown for the Rb, Th, Pb and La. 1. Mafic and intermediate volcanic rocks of the Transcarpathian Basin (Downes et al. 1995; Seghedi et al. 2001, 2004); 2. Quartz andesite in the Baia Mare region (Jurje et al. 2014); 3. Felsic volcanic rocks in the Transcarpathian Basin (Downes et al. 1995; Seghedi et al. 2001, 2004); 4. mafic enclave, andesite and dacite analyses of Laleaua Albă (Kovacs 2002, Seghedi et al. 2004; this study); 5. Melt inclusions (this study)

## Discussion

### *Melt composition parental to the phenocrysts*

Experiments attest that quartz crystallization from magmatic melt suggests a high water pressure that was no less than 8 kbar. This may imply a maximum initial storage depth for magma that led to melt inclusion entrapment at < 30 km, close to the crust-mantle boundary (Horváth et al. 2006). High-density inclusions of magmatic waters indicating high fluid pressure were earlier described from andesites and rhyolites of Slovakia and ignimbrites of the Lashkerek Massif in the Central Tien Shan (Naumov et al. 1991, 1992, 1994), rhyolites of New Zealand and the Rio Blanca Cu-Mo deposit of Chile (Davidson and Kamenetsky 2007).

The trace element chemical variation of the studied melt inclusions in quartz are all of similar composition and are relatively depleted compared to the whole rock data (Figs 15 and 16), being closer, from a geochemical point of view, to felsic rhyolites older than 10 Ma. This may suggest that the quartz was generated in earlier phases from acid melts.

The REE spider to chondrite of the melt inclusion shows an evident Eu anomaly typical for plagioclase fractionation. Such behavior was interpreted in the case of melt inclusions in quartz of Miocene rhyolites from the Pannonian Basin or the Dănești dacite as indicating entrapping in a stratified magma chamber at the upper crustal level (Lukács et al. 2005; Grancea et al. 2003).

However, petrographic observation of quartz crystals (corroded, sometimes with a pyroxene reaction rim, fissured and sometimes showing optical heterogeneity) and melt inclusion cryometric experiments for the Laleaua Albă dacite suggest that the quartz was formed at deeper levels in the crust. Crustal melting may have been triggered by an elevated temperature gradient caused by ascending andesitic magmas at the mantle-crust boundary; also, as suggested by the P-T conditions of such melts at ~ 8 Kbar, corresponding to ~30 km depth. On the other hand, the parental magmas of the mafic and intermediate samples appear to have been generated from an enriched heterogeneous source in the subcontinental lithospheric mantle (e.g. Seghedi et al. 2001, 2004). The discrepancy between some chemical compositions (e.g. the Eu anomaly in melt inclusions suggesting shallow crustal differentiation) and PT experiments (suggesting deeper origin) are difficult to reconcile without isotope data. The other possibility is a xenogenic origin for quartz crystals, which could have been trapped from volcanogenic wall-rocks. In this case it is easier to explain that quartz was formed during previous magmatic events from acid melts since it shows a similar geochemistry to the felsic rocks older than 10 Ma. However, the discrepancy between melt inclusion geochemistry, suggesting low-pressure fractionation, and experimentally suggested high pressure generation, still remains unexplained.

*Melt crystallization parameters*

The melt temperature of dacite was estimated using the amphibole-plagioclase thermometer (Holland and Blundy 1994). The compositions of plagioclase used in the calculations were selected according to the studied mineral zoning. The most calcic plagioclase was taken as being in equilibrium composition to the amphibole cores, while Pl 55 and Pl 35 were selected as being in equilibrium with the transitional zone and the rim of the amphibole, respectively. Pressure was calculated using the amphibole geobarometer (Anderson and Smith 1995). Calculations are shown in Fig. 17. Phenocrysts crystallized within 810–880 °C. As temperature in the magma reservoir increased, pressure decreased from 4 to 2.2 kbar. The minimum storage depth for the magma is suggested to be at about 8 km (from lithostatic pressure).

Somewhat different (higher) temperatures and pressures were calculated using the universal amphibole thermometer-barometer (Ridolfi et al. 2010). In this version of calculations the decrease in pressure (from core to rim in amphibole phenocrysts) from 6 to 4 kbar is accompanied by a decrease of crystallization temperature from 1050 to 960 °C. This would imply magma storage at 20–27 depth. Kovacs (2010), based on Al-inhornblende and amphibole-plagioclase barometers of mafic anclaves, suggests a depth of 18–25 km for their generation.

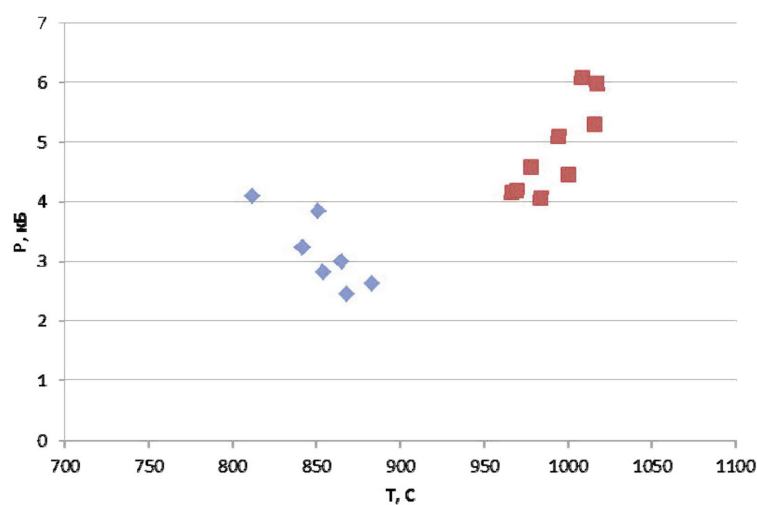


Fig. 17

PT conditions of amphibole-plagioclase phenocryst growth in dacite.

Diamonds show temperature determined using the Amph-Pl thermometer (Holland and Blundy 1994) and pressure calculated from the amphibole geobarometer (Anderson and Smith 1995). Boxes-temperature and pressure estimated from amphibole thermometer (Ridolfi et al. 2010)

*Magmatic and ore fluid-forming processes.*

High-temperature and high-pressure aqueous fluids formed during degassing of silicic magma were established at many deposits around the world, thus supporting the participation of these magma fluids in hydrothermal ore formation. The fluid composition in the silicate melt inclusions and their water contents in Laleaua Albă show similarities with those from the Dănești dacite (Grancea et al. 2003) whose compositions of melt inclusions were related with advanced fractional crystallization caused by magma ascent to the subsurface crustal level. During this polybaric crystallization, quartz and plagioclase phenocrysts entrapped melts with a wide range of dissolved water (1–5 wt% H<sub>2</sub>O), as in the case of the Laleaua Albă dacite. The aluminum saturation index A/CNK of residual melt (entrapped as glass inclusions) could have played a decisive role in ore generation, because the chemical composition of these melts is determined by the composition of exsolved magmatic-hydrothermal fluid. Experimental data on the Cl/fluid/melt partition coefficient show that  $D_{\text{fl/melt}}^{\text{Cl}}$  reaches maximal values in metaluminous melts and decreases in plumbite and apatitic magmas (Shinohara et al. 1989; Webster 1992). In addition, preliminary experimental studies of partitioning of non-ferrous metals (Pb, Zn) (Urabe 1985) between the magmatic volatile phase and coexisting granitic melt also indicate that the A/CNK index of melt may affect the  $D_{\text{fl/melt}}$  partition coefficient. We agree with Grancea et al. (2003) that fluids produced during magma degassing were able to extract significant amounts of chloride-related metals from the magmas and allow generation of ore deposits in the Baia Mare district. It is most probable that a similar kind of intrusion as Laleaua Albă, suggesting developed fractional crystallization and mixing, to have played a major role in the ore generation in the Baia Sprie district. We are taking into consideration the spatial association and the time of emplacement of Laleaua Albă similar with those of mineralization (~9–8 Ma) (e.g. Kovacs et al. 1997).

*Magma mixing processes*

Many petrological features of the dacite suggest disequilibrium attributed to the effect of magma mixing/mingling processes (Kovacs 2002; Kovacs et al. 2010; 2013; Kovacs and Fülöp 2010).

The formation of opacite rims around amphibole and biotite phenocrysts may indicate a sharp change in melt generation conditions. Usually opacitization is related to a decrease in H<sub>2</sub>O pressure (Rutherford and Devine 2003) or due to increasing temperature (Plechov et al. 2008). The generation of orthopyroxene in late assemblages testifies that opacitization was caused by increase in melt temperature. As demonstrated by experimental work (Johannes et al. 1994; Nakamura and Shimakita 1998), the porous (sieve) texture discernible in plagioclase phenocrysts also points to an increase in melt temperature and,

consequently, to the partial dissolution of sodic plagioclase with formation of this peculiar sieve texture.

The crystallization of orthopyroxene after formation of opacite rims around amphibole and biotite unambiguously indicates an increase of melt temperature. The temperatures of late granitic assemblage calculated from the two-feldspar thermometer (Fuhrman and Lindsley 1988) are 830 °C at 4 kbar and 784 °C at 2 kbar, which is significantly lower than the crystallization temperatures of amphibole-plagioclase phenocrysts. Hence an increase in temperature is presumably related to the hot, "dry", more basic melts (see the increase of An at the Pl margins), which were injected prior to the formation of the dacite groundmass and were responsible for the formation of the "post-opacite" phenocryst assemblage – Opx + Pl<sub>66</sub> + Ti-mgt.

Some of the disequilibrium features (resorbed quartz with pyroxene reaction rim in andesite and sieve texture; Kovacs 2002) could also be a consequence of decompression and degassing. The location of the magma mixing is unclear, but can be assumed to have been at the upper crustal level.

According to the petrology and compositions of the dacites together with the water and volatile contents inferred from melt inclusions, a development of a shallow, open-system magma is indicated. Disequilibrium textures in the dacite can be related to magma mixing, decompression related to magma ascent and eruption chambers at a few kms depth. According to the geochemical data the dacites were formed by mixing of an strongly fractionated felsic magma, more enriched and different from felsic magmas older than 10 Ma (see Figs 15, 16), with a primitive andesite magma as suggested by disrupted diorite-gabbro cumulates (similar to the suggested lithospheric magma in the area); mixing was most probably responsible for the eruption processes.

There still remains the problem of the Laleaua Albă quartz (possibly inherited?) that shows compositional similarities to felsic magmas older than 10 Ma, and not to the assumed younger 8–8.5 Ma hypothetical enriched felsic magma that may have contributed to the mixing/mingling processes.

### **Conclusions**

The following conclusions can be drawn from results obtained in this work:

1. Crystalline and melt inclusions were studied in quartz phenocrysts from the Laleaua Albă dacite. Crystalline inclusions are represented by plagioclase (An<sub>49–39</sub>), biotite (with F content up to 0.41 wt% and Cl up to 0.19 wt%) and magnetite (TiO<sub>2</sub> = 5.9–7.0 wt%, MnO = 0.9–1.7 wt%). Microprobe analysis of 29 melt inclusions in plagioclase, K-feldspar, and quartz allowed us to determine the average composition of the magmatic melt as follows (in wt%): 72.34 SiO<sub>2</sub>, 0.07 TiO<sub>2</sub>, 12.58 Al<sub>2</sub>O<sub>3</sub>, 0.60 FeO, 0.07 MnO, 0.07 MgO, 0.90 CaO, 3.50 Na<sub>2</sub>O, 5.13 K<sub>2</sub>O, 0.06 P<sub>2</sub>O<sub>5</sub>, 0.12 Cl, 0.07 F, 0.01 S. These data indicate that phenocrysts crystallized from silicic melts with K predominance over Na (K<sub>2</sub>O/Na<sub>2</sub>O = 1.5).

2. Based on the average total of components in microprobe analyses of 95.5 wt%, the average water content in the melt was 4.5 wt%. Judging from variations of this parameter from 92 to 99 wt%, the water content during crystallization of phenocrysts varied from 8 to 1 wt%.

3. Ion microprobe analysis (water and trace elements) of 11 melt inclusions showed that the lowest and the highest H<sub>2</sub>O contents in a glass of melt inclusions are 0.5 and 6.1 wt%, with an average content of 3.5 wt%, which is very consistent with the above-mentioned estimates of water content determined from microprobe analyses. Allowing for the high-density water of fluid segregation in one of melt inclusions, the water content in the melt could reach 84 wt%.

4. Ion microprobe data revealed high concentrations of Cu (up to 345–1260 ppm) as well as higher U content (from 5.0 to 14.3 ppm; average 11.5 ppm) in some melt inclusions as compared to the average U contents in silicic melts (2.7 ppm in island-arc settings and 79 ppm in continental rift settings according to Naumov et al. 2010b).

5. Chondrite-normalized trace-element patterns in melt inclusions suggest a complex genesis of the studied magmatic melts. The contents of some elements (for instance, Sr and Ba) are close to those in island-arc melts, while others (for instance, Th, U, and Eu) resemble those in melts of continental settings.

### Acknowledgements

The studies were carried out within the framework of the Joint Project "Interrelations between geodynamic evolution and magmatism as fundamental factors of origination and evolution of ore-forming systems in the volcanic regions of Romania during the Miocene" of the IGEM RAS and the Institute of Geodynamics of the Romanian Academy, and were financially supported by the Russian Foundation for Basic Research (project nos. 13-05-00622a, 13-05-00450a and 12-05-01083a).

We are grateful to N. N. Kononkova, A. I. Yakushev, and K. V. Van for help in analytical studies. We thank Vadim S. Kamenetsky and Maxim Portnyagin for their constructive comments.

### References

- Anderson, J.L., D.R. Smith 1995: The effect of temperature and oxygen fugacity on Al-in-hornblende barometry. – *Amer. Mineralogist*, 80, pp. 549–559.
- Audetat, A., D. Gunther 1999: Mobility and H<sub>2</sub>O loss from fluid inclusions in natural quartz crystals. – *Contrib. Mineral. Petrol.*, 137, pp. 1–14.
- Borcoş, M. 1994: Neogene volcanicity/metallogeny in the Oaş-Gutâi Mts. – In: Borcoş M, Ş. Vlad (Eds): IGCP 356 fieldtrip guide, Conf. Plate Tectonics and Metallogeny in the East Carpathians and Apuseni Mts., Bucharest, pp. 20–22.
- Borcoş, M., B. Lang, S. Boştinescu, I. Gheorghişă 1995: Neogene hydrothermal ore deposits in the volcanic Gutâi Mountains, part III. – *Rev. Roum. Geol., Geophys., Geogr. Ser. Geol.*, 19, pp. 21–35.

- Crahmaliuc, R., J. Andrei, A. Crahmaliuc 1995: The magnetic modelling of the Gutai Neogene plutonic body. – *Rom. J. Stratig.*, 76, 7, pp. 63–64.
- Csontos, L., E. Márton, G. Wórum, L. Benkovics 2002: Geodynamics of SW-Pannonian inselbergs (Mecsek and Villány Mts, SW Hungary). – *EGU Stephan Mueller Special Publication* 3, pp. 227–245.
- Damian, G., L. Nedelcu, D. Istvan 1995: Two representative vein deposits (Au-Ag and Pb-Zn) related to Neogene volcanic structures. – In: Udubasa, G. (Ed): *Minerals and mineral occurrences in the Baia Mare district. Excursion guides*. *Rom. J. Mineral*, 77/2, pp. 21–43.
- Davidson, P., V.S. Kamenetsky 2007: Primary aqueous fluids in rhyolitic magmas: Melt inclusion evidence for pre- and post-trapping exsolution. – *Chemical Geology*, 237, pp. 372–383.
- Downes, H., G. Pantó, T. Póka, D.P. Matthey, P.B. Greenwood 1995: Calc-alkaline volcanics of the Inner Carpathian arc, Northern Hungary: new geochemical and oxygen isotopic results. – *Acta Vulcanologica*, 7, pp. 29–41.
- Edelstein, O., A. Bernard, M. Kovacs, M. Crihan, Z. Pécskay 1992: Preliminary date regarding the K-Ar ages of some eruptive rocks from Baia Mare Neogene volcanic zone. – *Rev. Roum. de Geol.*, 36, pp. 45–60.
- Edelstein, O., Z. Pécskay, M. Kovacs, A. Bernad, M. Crihan, R. Micle 1993: The age of the basalts of the Firiza zone, Igriș Mts., East Carpathians, Romania. – *Rev. Roum. Geol.*, 37, pp. 45–60.
- Fodor, L., L. Csontos, G. Bada, I. Györfi, L. Benkovics 1999: Cenozoic tectonic evolution of the Pannonian basin system and neighboring orogens: a new synthesis of paleostress data. – In: Durand, B., L. Jolivet, F. Horváth, M. Séranne (Eds): *The Mediterranean basins: Cenozoic Extension within the Alpine Orogen*. *Geological Society Special Publication* 156, pp. 295–334.
- Frezzotti, M.-L. 2001: Silicate-melt inclusions in magmatic rocks: applications to petrology. – *Lithos*, 55, pp. 273–299.
- Fuhrman, M.L., D.L. Lindsley 1988: Ternary-feldspar modeling and thermometry. – *American Mineral.*, 73/3–4, pp. 201–215.
- Garcia, M.O., S.S. Jacobson 1979: Crystal clots, amphibole fractionation and the evolution of calc-alkaline magmas. – *Contrib. Mineral. Petrol.*, 69, pp. 319–327.
- Grancea, L., A. Fülöp, M. Cuney, J. Leroy, J. Pironon 2003: Magmatic evolution and ore-forming fluids involved in the origin of the gold/base metals mineralization in the Baia Mare province, Romania. – *J. Geochem. Explor.*, 78/79, pp. 627–630.
- Halter, W.E., C.A. Heinrich, T. Pettke 2004: Laser-ablation ICP-MS analysis of silicate and sulfide melt inclusions in an andesitic complex II: magmas genesis and implications for ore-formation. – *Contrib. Mineral. Petrol.*, 147, pp. 397–412.
- Halter, W.E., C. Heinrich, T. Pettke 2005: Magma evolution and the formation of porphyry Cu-Au ore fluids: Evidence from silicate and sulfide melt inclusions. – *Mineralium Deposita*, 39, pp. 845–863.
- Harris, A.C., V.S. Kamenetsky, N.C. White, E. van Achterberg, C.G. Ryan 2003: Melt inclusion in veins: Linking magmas and porphyry Cu deposits. – *Science*, 32, pp. 2109–2111.
- Holland, T.J.B., J.D. Blundy 1994: Non-ideal interactions in calcic amphiboles and their bearing on amphibole-plagioclase thermometry. – *Contrib. Mineral. Petrol.*, 116, pp. 433–447.
- Horváth, F., G. Bada, P. Szafián, G. Tari, A. Ádám, S. Cloetingh 2006: Formation and deformation of the Pannonian Basin: constraints from observational data. – In: Gee, D.G., R. Stephenson (Eds): *European Lithosphere dynamics*, *Geological Society London Memoir*, 32, pp. 191–206.
- Johannes, W., J. Koepke, H. Behrens 1994: Partial melting reactions of plagioclase and plagioclase-bearing assemblages. – In: Parson, I. (Ed.): *Feldspars and their Reactions*. Kluwer, Dordrecht, pp. 161–194.
- Jurje, M., C. Ionescu, V. Hoeck, M. Kovacs 2014: Geochemistry of Neogene quartz andesites from the Oaş and Gutâi Mountains, Eastern Carpathians (Romania): a complex magma genesis. – *Miner. Petrol.*, 108, pp. 13–32.
- Kovacs, M. 2002: Petrogenesis of the subduction magmatic rocks from central-southeastern area of Gutâi Mountains. – *Edit. Dacia* 202 p. (In Romanian.)

- Kovacs, M., D. Istvan, A. Fülöp 1995: Neogene volcanism and associated metallogeny in the Oas-Gutai Mts. – In: Udubasa, G. (Ed.) Minerals and mineral occurrences in the Baia Mare district. Excursion guides. – Rom. J. Mineral., 77/2, pp. 21–43.
- Kovacs, M., O. Edelstein, M. Gabor 1997: Neogene magmatism and metallogeny in the Oas-Gutai-Tibles Mts.: a new approach based on radiometric datings. – Rom. J. Miner. Deposits, 78, pp. 35–45.
- Kovacs, M., Fülöp A., 2010: Stop 4: Laleaua Albă quarry: a Neogene composite igneous body. – In: Iancu, O.G., M. Kovacs (Eds): Ore deposits and other classic localities in the Eastern Carpathians: From metamorphics to volcanics. Acta Mineralogica-Petrographica, Field guide series, vol. 19, pp. 32–35.
- Kovacs, M., A. Fülöp, Z. Pécskay, M. Jurje 2013: Magma-mixing and -mingling as key magmatic processes controlling the development of the volcanic events in the Gutâi Neogene Volcanic Zone, Eastern Carpathians, Romania. – Abstract, IAVCEI 2013 Scientific Assembly. 180, 4W\_1D–P4.
- Kovalenker, V.A., V. Yu. Prokofiev, M. Haber, S. Jelen 1999: Banska Stiavnica epithermal fluid-magmatic system: fluid/salt melt inclusions studies. – Geologica Carpathica, 50, Special issue, pp. 188–189.
- Kovalenker, V.A., V.B. Naumov, V.Yu. Prokofiev, S. Jelen, M. Haber 2006: Compositions of Magmatic Melts and Evolution of Mineral-Forming Fluids in the Banska Stiavnica Epithermal Au-Ag-Pb-Zn Deposit, Slovakia: A Study of Inclusions in Minerals. – Geochemistry Int., 44/2, pp. 118–136.
- Lang, B., O. Edelstein, M. Kovacs, A. Bernad, M. Crihan, 1994: K-Ar age determination on Neogene volcanic rocks from Gutâi Mts (Eastern Carpathians, Romania). – Geologica Carpathica, 45/6. pp. 357–363.
- Lexa, J., I. Seghedi, K. Németh, A. Szakács, V. Konecný, Z. Pécskay, A. Fülöp, M. Kovacs 2010: Neogene–Quaternary volcanic forms in the Carpathian–Pannonian Region: a review. – Central European Journal of Geosciences, 2/3, pp. 207–270, DOI: 10.2478/v10085-010-0024-5.
- Lukács, R., Sz. Harangi, T. Ntaflos, P.R.D. Mason 2005: Silicate melt inclusions in the phenocrysts of the Szomolya Ignimbrite, Bükkalja Volcanic Field (Northern Hungary): Implications for magma chamber processes. – Chemical Geology, 223, pp. 46–67.
- Márton, E., M. Tischler, M. Csontos, B. Fügenschuh, S.M. Schmid 2007: The contact zone between the ALCAPA and Tisza–Dacia mega-tectonic units of Northern Romania in the light of new paleomagnetic data. – Swiss J. Geosciences, DOI 10.1007/s00015-007-1205-5.
- Milesi, J.P., M. Borcos, A. Genna, C. Stanciu, P. Piantone, J. Andrei, R. Crahmaliuc, E. Marcoux, B. Găbudeanu, O. Edelstein 1994: Geodynamic controls of epithermal mineralization in the Gutai Neogene volcanic region (Baia Mare, Romania). – In: Borcos, M., Ş. Vlad (Eds): IGCP 356, Field trip guide. Plate tectonics and metallogeny in the East Carpathians and Apuseni Mts., Bucharest, pp. 10–11.
- Mitchell, A.H.G. 1996: Distribution and genesis of some epizonal Zn-Pb and Au provinces in the Carpathian and Balkan region. – Trans. Inst. Min. Metall., 105, B. pp. 127–138.
- Nakamura, M., S. Shimakita 1998: Dissolution origin and syn-entrapment compositional change of melt inclusion in plagioclase. – Earth Planetary Science Letters, 161, pp. 119–133.
- Naumov, V.B., I.P. Solovova, V.A. Kovalenker, V.L. Rusinov, N.N. Kononkova 1991: Data on high density magmatic aqueous fluid inclusions in phenocrysts of rhyolite. – Dokl. Russ. Acad. Nauk, 318, 1, pp. 187–190. (In Russian.)
- Naumov, V.B., I.P. Solovova, V.A. Kovalenker, V.L. Rusinov, N.N. Kononkova 1992: Magmatic water under a pressure of 15–17 kbar and its concentration in melt: the first data on inclusions in plagioclases in andesites. – Dokl. Russ. Acad. Nauk, 324, 3, pp. 654–658. (In Russian.)
- Naumov, V.B., V.L. Rusinov, V.A. Kovalenker, N.N. Kononkova 1993: Melt composition, rare elements content, and formation conditions of the quartz from the Lashkerek ignimbrites massif according to the study of melt inclusions. – Dokl. Russ. Acad. Nauk, 332, 1, pp. 79–82. (In Russian.)

- Naumov, V.B., V.L. Rusinov, V.A. Kovalenker, N.N. Kononkova 1994: High pressure fluid inclusions of magmatic water in the phenocrysts of silicic volcanics in the Western Carpathians and the Middle Tien Shan. – *Petrology*, 2/5, pp. 480–494.
- Naumov, V.B., V.A. Kovalenker, V.L. Rusinov 2010a: Chemical Composition, Volatile Components, and Trace Elements in the Magmatic Melt of the Kurama Mining District, Middle Tien Shan: Evidence from the Investigation of Inclusions in Quartz. – *Geochemistry Int.*, 48, pp. 555–568.
- Naumov, V.B., V.I. Kovalenko, V.A. Dorofeeva, A.V. Girnis, V.V. Yarmolyuk 2010b: Average compositions of igneous melts from main geodynamic settings according to the investigation of melt inclusions in minerals and quenched glasses of rocks. – *Geochemistry Int.*, 48, pp. 1185–1207.
- Nosova, A.A., L.V. Sazonova, V.V. Narkisova, S.G. Simakin 2002: Minor elements in clinopyroxene from Paleozoic volcanics of the Tagil Island Arc in the Central Urals. – *Geochemistry Int.*, 40, pp. 219–232.
- Pécskay, Z., J. Lexa, A. Szakacs, Kad. Balogh, I. Seghedi, V. Konecny, M. Kovacs, E. Marton, V. Szeky-Fux, T. Poka, P. Gyarmaty, O. Edelstein, E. Rosu, B. Zec 1995: Space and time distribution of Neogene Quaternary volcanism in the Carpatho-Pannonian region. – *Acta Vulcanol.*, 7, pp. 15–29.
- Pécskay, Z., J. Lexa, A. Szakács, I. Seghedi, K. Balogh, V. Konecný, T. Zelenka, M. Kovacs, T. Póka, A. Fülöp, E. Márton, C. Panaiotu, V. Cvetkovic, V. 2006: Geochronology of Neogene–Quaternary magmatism in the Carpathian arc and Intra–Carpathian area: a review. – *Geologica Carpathica*, 57, pp. 511–530.
- Plechov, P.Yu., T.A. Shishkina, V.A. Ermakov, M.V. Portnyagin 2008: Formation conditions of allivalites, olivine-anorthite crystal enclaves, in the volcanics of the Kuril-Kamchatka arc. – *Petrology*, 16, pp. 232–260.
- Portnyagin, M.V., S.G. Simakin, A.V. Sobolev 2002: Fluorine in primitive magmas of the Troodos ophiolite complex, Cyprus: Analytical methods and main results. – *Geochemistry Int.*, 40, pp. 625–632.
- Prokofiev, V.Yu., V.S. Kamenetsky, V.A. Kovalenker, S.B. Bodon, S. Jelen 1999: Evolution of magmatic fluids at Banska Stiavnica precious and base metal deposit, Slovakia – Evidence from melt and fluid inclusions. – *Economic Geology*, 94/6, pp. 949–956.
- Ridolfi, E., A. Rezzulli, M. Puerini 2010: Stability and chemical equilibrium of amphibole in calc-alkaline magmas: an overview, new thermobarometric formulations and application to subduction-related volcanoes. – *Contrib. Mineral. Petrol.*, 160, pp. 45–66.
- Royden, L.H. 1988: Late Cenozoic tectonics of the Pannonian Basin system. – In: Royden, L.H., F. Horváth (Eds): *The Pannonian Basin. A Study in Basin evolution*, AAPG Memoir 45. The American Association of Petroleum Geologists and the Hungarian Geological Society, Tulsa, Budapest, pp. 27–48.
- Rutherford, M.J., J.D. Devine 2003: Magmatic conditions and magma ascent as indicated by hornblende phase equilibria and reactions in the 1995–2002 Soufriere Hills magma. – *J. Petrology*, 44, pp. 1433–1454.
- Săndulescu, M. 1988: Cenozoic tectonic history of the Carpathians. – In: Royden, L.H., F. Horváth (Eds): *The Pannonian Basin: A Study in Basin Evolution*. AAPG Memoir., 45, pp. 17–25.
- Săndulescu, M., M. Visarion, D. Stănică, M. Stănică, L. Atanasiu 1993: Deep structure of the inner Carpathians in the Maramures–Tisa zone (East Carpathians). – *Rom. J. Geophysics*, 16, pp. 67–76.
- Schmid, S., D. Bernoulli, B. Fügenschuh, L. Mañenco, S. Schefer, R. Schuster, M. Tischler, K. Ustaszewski 2008: The Alpine–Carpathian–Dinaridic orogenic system: correlation and evolution of tectonic units. – *Swiss J. Geosciences*, doi: 10.1007/s00015-008-1247-3, pp. 139–183.
- Seghedi, I., I. Balintoni, A. Szakács 1998: Interplay of tectonics and Neogene post-collisional magmatism in the Intracarpathian area. – *Lithos*, 45, pp. 483–499.
- Seghedi, I., H. Downes, Z. Pécskay, M.F. Thirlwall, A. Szakács, M. Prychodko, D. Matthey 2001: Magmatogenesis in a subduction-related post-collisional volcanic arc segment: the Ukrainian Carpathians. – *Lithos*, 57, pp. 237–262.

- Seghedi, I., H. Downes, A. Szakács, T.R.D. Mason, M.F. Thirlwall, E. Roşu, Z. Pécskay, E. Márton, C. Panaiotu 2004: Neogene–Quaternary magmatism and geodynamics in the Carpathian–Pannonian region: a synthesis. – *Lithos*, 72, pp. 117–146.
- Seghedi, I., H. Downes 2011: Geochemistry and tectonic development of Cenozoic magmatism in the Carpathian–Pannonian region. – *Gondwana Research*, 20, pp. 655–672.
- Shinohara, H., J.T. Iiyama, S. Matsuo 1989: Partitioning of chlorine compounds between silicate melt and hydrothermal solutions: I. Partition of Na-KCl. – *Geochim. Cosmochim. Acta*, 53, pp. 2617–2630.
- Simmons, S.F., N.C. White, D.A. John 2005: Geological characteristics of epithermal precious and base metal deposits. – *Economic Geology*, 100, pp. 485–522.
- Sobolev, A.V. 1996: Melt inclusions in minerals as a source of principle petrological information. – *Petrology*, 4/3, pp. 209–220.
- Soták, J., A. Biron, R. Prokešova, J. Spišák 2000: Detachment control of core complex exhumation and back-arc extension: case study from East Slovak basin. – *Geolines*, 10, pp. 66–67.
- Sun, S., W.F. McDonough 1989: Chemical and isotopic systematics of oceanic basalts: implications for mantle composition and processes. – In: Saunders, A.D., M.J. Norry (Eds): *Magmatism in the Oceanic Basins*. V. 42. Geological Society, pp. 313–345.
- Szakács, A., Z. Pécskay, L. Silye, K. Balogh, D. Vlad, A. Fülöp 2012: On the age of the Dej Tuff, Transylvanian Basin (Romania). – *Geologica Carpathica*, 63, pp. 139–148.
- Urabe, T. 1985: Aluminous granite as source magma of hydrothermal ore deposits: an experimental study. – *Econ. Geol.*, 80, pp. 148–157.
- Wallier, S., R. Rey, K. Kouzmanov, T. Pettke, C.A. Heinrich, S. Leary, G. O'Connor, G., C.G. Tămas, T. Vennemann, T. Ulrich 2006: Magmatic fluids in the breccia-hosted epithermal Au-Ag deposit of Rosia Montana, Romania. – *Econ. Geol.*, 101, pp. 923–954.
- Webster, J.D. 1992: Fluid-melt interactions involving Cl-rich granites: experimental study from 2 to 8 kbar. – *Geochim. Cosmochim. Acta*, 56, pp. 659–678.